Research Article

Hara Jeon, Lee Ku Kwac, Hong Gun Kim, and Jin-Hae Chang*

Comparison of properties of colorless and transparent polyimide films using various diamine monomers

https://doi.org/10.1515/rams-2022-0044 received February 14, 2022; accepted June 12, 2022

Abstract: Six different types of polyamic acids were synthesized by reacting 1,2,4,5-cyclohexanetetracarboxylic dianhydride with the diamine monomers 3,4-oxydianiline, 1,3-bis(3-aminopheno-xy)benzene, 1,4-bis(4-amino-phenoxy)benzene, *m*-bis[4-(3-aminophenoxy)phenyl]sulfone, p-bis[4-(4-aminophenoxy)-phenyl]sulfone, and 2,2-bis[4-(4-aminophenoxy)phenyl]hexafluoropropane. Thereafter, polyimide (PI) films were prepared via various heat treatment processes. The diamine monomers used in this study for the synthesis of colorless and transparent PI (CPI) were characterized by a bent meta-structure or a para-linear chain containing ether (-0-) bonds. In addition, some monomers included fluorine (-CF₃) substituents and sulfone (-SO₂-) groups. Furthermore, the thermal and mechanical properties, optical transparency, and solubility of the CPI films with six different diamine monomer structures were investigated. The correlation between CPI film properties and related monomer structures was specifically emphasized.

Keywords: colorless and transparent polyimide, film, thermo-mechanical properties, optical transparency

1 Introduction

Owing to their excellent thermo-mechanical properties, chemical resistance, and transparency, polyimide (PI)

* Corresponding author: Jin-Hae Chang, Institute of Carbon Technology, Jeonju University, Jeonju 55069, Korea, e-mail: changjinhae@hanmail.net

Hara Jeon: Graduate School of Carbon Convergence Engineering, Jeoniu University, Jeoniu 55069, Korea

Lee Ku Kwac, Hong Gun Kim: Graduate School of Carbon Convergence Engineering, Jeonju University, Jeonju 55069, Korea; Institute of Carbon Technology, Jeonju University, Jeonju 55069, Korea and PI-based composite films are widely used in precision applications in various industries including the aerospace, aviation, and automotive industries [1–4]. Recently, the flexibility, lightweight, and excellent thermal properties of PI have been exploited to fabricate electronics and solar panels. Furthermore, highly flexible PI composite materials with excellent processability can be used for electromagnetic interference shielding applications or as conductive polymer materials to replace metals, which have been widely used thus far in device fabrication [5,6]. Despite their various advantages, dark brown-colored PI films have limited practical applications in the field of flexible displays, as they cannot replace colorless and transparent glass in electronic devices [3,4].

The dark brown color of PI films results from a charge transfer complex (CTC) arising from the π electrons of the imide main chain [7,8]. Diverse methods are typically used to convert these films into colorless, transparent PI (CPI) films [9,10]. These methods include the following: (1) introducing a strong electron-attracting group, such as trifluoromethyl ($-CF_3$) or sulfone ($-SO_2-$), owing to its electronegativity; (2) introducing an ether (-0-) group capable of free rotation into the main chain to form a relatively flexible structure; (3) designing an overall curved structure to limit the movement of π electrons, thereby reducing the CTC effect. Engineering plastic films such as polyethylene terephthalate, polycarbonate, and poly methyl methacrylate have been widely used in the field of optical organic materials owing to their high optical transmittance, which is greater than 80% at ~400 nm. Nonetheless, their low glass transition temperature ($T_{\rm g}$ < 150°C) hinders their applications at high temperatures [3,11,12].

Until now, most of the dianhydride monomer structures for the CPI synthesis were composed of benzene or comparable aromatic structures and double bonds. In particular, benzene structures were introduced to impart heat resistance, suitable mechanical properties, and chemical resistance to the synthesized films. However, benzene-based CPI film processing is hindered by the low solubility of such films and posttreatment difficulties.

Moreover, π electrons in the aromatic benzene component absorb light to some extent in the visible light region, causing the dark brown or yellow color in CPI films.

Alicyclic monomer structures are occasionally used to improve the optical properties of CPI films and to hinder the CTC. Monomer structures used for alicyclic CPI include trans-1,4-cyclohexanediamine [13], 4,4'-methylenebis-(2-methylcyclohexyamine) [14], bicyclo(2,2,2)-oct-7-ene-2,3,5,6-tetracarboxylic dianhydride [15,16], 1,2,3,4-cyclobutanetetracarboxylic dianhydride [17], and 1,2,4,5-cyclohexanetetracarboxylic dianhydride (CHDA) [17]. These alicyclic structures in the main CPI chain lead to physicochemical properties comparable to those of benzene. In addition, alicyclic CPI films are processed at high temperatures of up to 300°C to enhance their flexibility and toughness while ensuring a low color and high transparency.

CPI can be widely applied to electronic devices as display glass. Moreover, due to its facile synthesis and mass production possibilities, it can be used for plasma display panels, liquid crystal displays, and solar panels, which are in the spotlight as alternative energy sources [3,18-20]. Recently, flexible and transparent materials such as indium tin oxide, characterized by a conductive oxide layer, have been extensively used in the fields of display substrates and microelectronics [21-23]. However, since indium is a rare and expensive element, it represents a strategic global commodity, causing difficulties in international transactions. An additional restriction on its use as a display material is glass plate processing at high temperatures to obtain a high purity, which results in fragility and lack of flexibility [22,23]. Therefore, CPI is a suitable alternative to overcome the limitations of glass. More interestingly. CPI films can be used as rollable transparent electrodes for wearable electronic devices [24,25].

In this study, CHDA replaced the conventional benzene structure. In fact, CHDA has the effect of increasing the transparency of the film by interfering with the formation of CTC during the synthesis reaction. In particular, Mitsubishi Gas Chemical Company used CHDA as a monomer to synthesize CPI films with excellent optical properties [26,27]. PI resin, commercially known as Neopulim[®], was prepared from CHDA and aromatic diamines by one-step high-temperature polycondensation. The six diamines used in this study have a bent meta-structure and -CF₃ or -SO₂- groups in the main chain, which is a structure that has the potential to exhibit the characteristics of CPI.

The present study aimed to synthesize new CPIs linked by ether linkages using two groups of diamines and to investigate the correlation between the structural

and physical properties of the synthesized CPIs. The first group had only one ether bond without substituents in the main chain, and the whole structure was substituted in a meta-form. The second group of monomers contained highly electronegative and highly polar -CF₃ and -SO₂- substituents in the main chain. The thermal properties, thermal stability, and oxygen permeability of the CPI films, each having one of six different monomer structures, were investigated. Furthermore, mechanical tensile properties, optical transparency, and solubility were investigated. The correlation between CPI properties and their corresponding monomer structures was elucidated, and their results were compared.

2 Experimental

2.1 Materials

Six diamine monomers including CHDA were purchased from TCI (Tokyo, Japan). The solvent, N,N'-dimethyl acetamide (DMAc) provided by Sigma-Aldrich (Yongin, Korea), was used after complete moisture removal.

2.2 Synthesis of CPI films

Scheme 1 shows the polyamic acids (PAAs) and CPI synthetic route starting from the reaction of various diamine monomers with CHDA. The procedure was the same for all monomers, which had different chemical structures. In this study, only the synthesis using 3,4-oxydianiline (3,4-ODA) will be described. CHDA (2.91 g, 1.3×10^{-2} mole) was completely dissolved in DMAc (12 mL) using a 100 mL three-necked flask by stirring for 30 min. Then, 3,4-ODA (2.60 g, 1.3×10^{-2} mole) was added to the CHDA solution. After a 1 h reaction at 0°C under nitrogen atmosphere, the reaction was performed at room temperature for 14 h to obtain a PAA solution. The obtained PAA solution was evenly spread on a clean glass plate and maintained in vacuum at 50°C for 1 h until stabilization. The solvent was further removed by maintaining the solution at 80°C in a vacuum for another hour. For complete imide reaction, PAA was heated in nitrogen atmosphere at 110, 140, 170, 200, 230, and 250°C for 30 min. Detailed heat treatment conditions are summarized in Table 1. Each synthesized CPI film was immersed in a 5 wt% hydrofluoric acid aqueous solution and slowly removed from the glass plate. The film was obtained with a size of up to

p-BAPB

VI

Scheme 1: Synthetic routes for CPI films based on CHDA monomer.

3,4-ODA

Table 1: Heat treatment conditions of the CPI films obtained from the CHDA monomer

Sample	Temperature (°C)/time (h)/pressure (Torr)
PAA CPI	$0/1/760 \rightarrow 25/14/760 \rightarrow 50/1/1 \rightarrow 80/1/1$ $110/0.5/760 \rightarrow 140/0.5/760 \rightarrow 170/0.5/760 \rightarrow$
	$200/0.5/760 \rightarrow 230/0.5/760 \rightarrow 250/0.5/760$

 $10 \text{ cm} \times 10 \text{ cm}$. Except for CPI using 3,4-ODA, all the synthesized CPI films were soluble in DMAc, with a solution viscosity in the range of 0.77-0.91 dL·g⁻¹ (see Table 2).

2.3 Characterization

Fourier transform infrared (FT-IR) spectroscopy (PerkinElmer, L1600300, London, UK) was used to investigate functional group absorption peaks to confirm the completed synthesis of CPI films. Moreover, nuclear magnetic resonance (NMR) chemical shifts of PI films were measured using a Bruker 400 MHz Avance II + NMR spectrometer (Bruker, Berlin, Germany). The Larmor frequency for ^1H magicangle spinning (MAS) NMR was $\omega_{\text{O}}/2\pi=400.13\,\text{MHz},$ and that for the ^{13}C MAS NMR experiment was $\omega_{\text{O}}/2\pi=100.61\,\text{MHz}$. To minimize spinning sidebands, MAS speeds for ^1H and ^{13}C were measured at 12–14 kHz. NMR peaks were referred to tetramethylsilane signal.

Differential scanning calorimetry (DSC; NETZSCH 200F3, Berlin, Germany) and thermo gravimetric analyzer (TGA; TA instrument TA Q-500, New Castle, USA) were used to investigate the thermal properties of the prepared CPI films. The coefficient of thermal expansion (CTE) was measured with a thermo-mechanical analyzer (TMA; TA instrument TMA2940, Seiko, Tokyo, Japan) in the temperature range between 50 and 150°C. The Chemdraw Office[®] program was used to analyze the three-dimensional polymer chain structure.

To measure the oxygen transmission rate (O_2TR) of the films, a MOCON, OX-TRAN 2/61 (Minneapolis, USA), was used, following the ASTM D3985 standard test method. Experimental conditions were set to 100% O_2 concentration and 0% relative humidity at a temperature of 23°C. Mechanical properties were measured with a universal tensile machine (UTM; Instron model 5564, Shimadzu, Japan), and the sample (5 mm \times 70 mm) was used at a crosshead speed of 5 mm·min⁻¹.

To investigate the optical transparency, an ultraviolet/visible spectrophotometer (UV-Vis. SHIMADZU UV-3600, Tokyo, Japan) and a color difference meter (KONICA MINOLTA CM-3600D, Tokyo, Japan) were used. Film thickness in the range $68-74\,\mu m$ enabled the comparison of physical properties.

Table 2: General properties of CPI films obtained from the CHDA monomer

СРІ	Thickness (µm)	I.V. ^a (dL·g ⁻¹)	T _g (°C)	<i>T</i> ^{<i>i</i> b} (°C)	wt _R ^{600c} (%)	CTE ^d (ppm⋅°C ⁻¹)	O ₂ TR ^e (cc·m ⁻² ·day ⁻¹)
1	70	Insol ^f	199	469	42	47.74	1.88
II	74	0.90	182	449	41	52.61	2.62
Ш	68	0.77	210	469	43	51.41	0.63
IV	74	0.87	190	452	46	45.43	1.50
V	72	0.83	225	451	42	48.68	0.39
VI	71	0.91	223	473	48	60.37	13.69

^aInherent viscosity was measured at 30°C by using a $0.1\,\mathrm{g}\cdot100\,\mathrm{mL}^{-1}$ solution in a *N,N'*-dimethylacetamide. ^bAt 2% initial weight-loss temperature. ^cWeight percent of residue at 600°C. ^dThe CTE temperature range was 50–150°C. ^eO₂TR. ^fInsoluble.

3 Results and discussion

3.1 FT-IR

Since all monomer structures were reacted with the same dianhydride, only the FT-IR result for structure I (see Scheme 1) is shown in Figure 1. Specifically, C=O stretching peaks at 1,785 and 1,731 cm⁻¹ and the characteristic imide peak corresponding to C-N-C stretching at 1,367 cm⁻¹ confirmed the PI synthesis [28]. More detailed peak information is summarized in Table 3.

To determine whether PAA changed to PI under various heat treatment conditions, the PI structure according to the imidization process was traced based on the functional group peak, as shown in Figure 1. In PAA, under the 50°C heat treatment condition, an amide C=O stretching peak at 1,684 cm⁻¹ (peak d) and an amide NH bending peak at 1,536 cm⁻¹ (peak b) were observed. However, the two peaks disappeared as the heat treatment temperature increased. In addition, the intensity of the C=O stretching peaks observed at 1,785 cm⁻¹ (f) and 1,731 cm⁻¹ (e) and the C-N-C stretching peak observed at 1,367 cm⁻¹ (a) increased gradually as the annealing temperature increased to 250°C. It is thus possible to confirm that the imidization reaction of PAA occurred at the various heat treatment temperatures.

3.2 ¹H MAS NMR and ¹³C MAS NMR

¹H MAS NMR was used to confirm the structure of the synthesized PI. For example, structure I synthesized using

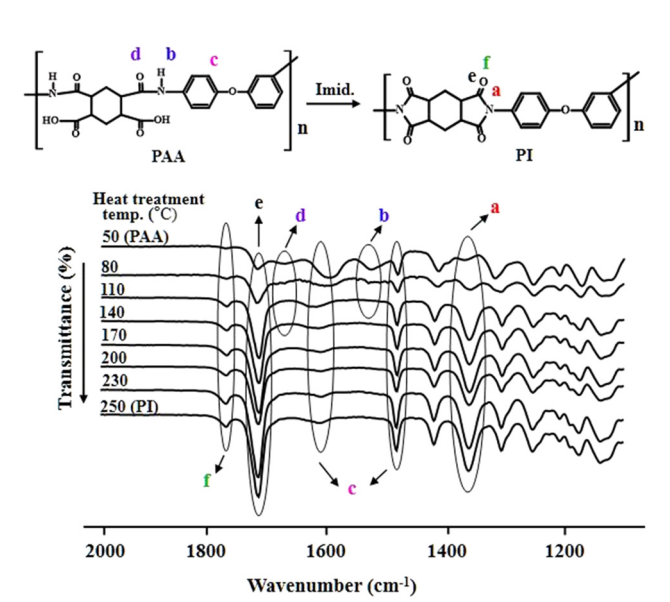


Figure 1: FT-IR spectra of PI as a function of various heat treatment temperatures.

Table 3: FT-IR peak assignments for PI film

Peak	Wavenumber (cm ⁻¹)	Peak assignment
a	1,367	C-N-C stretching of imide ring
b	1,536	N-H bend of amide
С	1,491, 1,622	C=C stretching of benzene
d	1,684	C=0 stretching of amide
е	1,731	Symmetric C=0 stretching of imide
f	1,785	Asymmetric C=0 stretching of imide

CHDA and 3,4-ODA monomers was confirmed and is shown in Figure 2. PI was insoluble in general NMR solvents; therefore, solid-state ¹H MAS NMR was used. Further, in the chemical structure shown in Figure 2, hydrogen of the aromatic ring appear at 8.00 ppm and those of the aliphatic ring show an overlapping peak at 3.95 ppm [29].

Solid-state ¹³C MAS NMR was used to confirm the structure with a double cross check. The chemical shift of benzene and aliphatic rings contained in CPI films was investigated by ¹³C MAS NMR at room temperature (Figure 3). Signals corresponding to benzene carbon atoms were detected at 121.59, 128.78, 133.01, 154.99, and 158.54 ppm, whereas a very strong C=O group was observed at 178.48 ppm. Peaks at 21.31 and 38.16 ppm correspond to the aliphatic rings [29]. The NMR results confirmed structure I achievement.

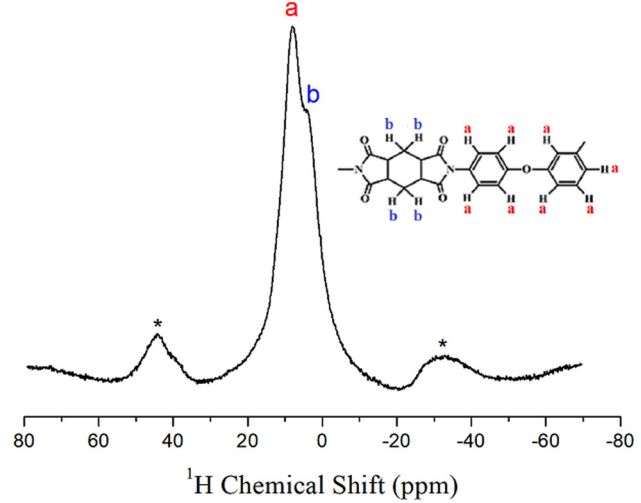


Figure 2: ¹H MAS NMR spectrum of the CPI film obtained by the reaction of CHDA with 3,4-ODA. The spinning sidebands for the aliphatic ring are marked with asterisks (*).

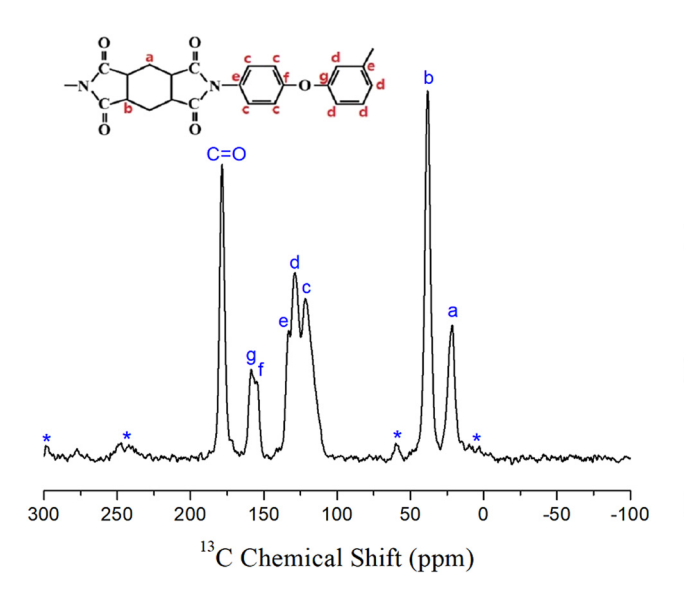


Figure 3: ¹³C MAS NMR spectrum of the CPI film obtained by the reaction of CHDA with 3,4-ODA. The spinning sidebands for the benzene ring and C=O are marked with asterisks (*).

3.3 Thermal properties

Table 2 summarizes the CPI T_g values obtained for various monomers. Generally, $T_{\rm g}$ depends on the polymer chain rigidity and the free volume required for the polymer chain to move [30–33]. Depending on the monomer structure, T_g of the related polymers varied in the range of 182-225°C. To clarify the correlation between properties and structure of the synthesized CPI films, Figure 4 shows the three-dimensional polymer structure. Structure I in Scheme 1 showed an overall linear structure, with $T_{\rm g}$ of 199°C (see Figure 4). While the structures of isomers II and III were analogous (Scheme 1), structure II formed a bent meta-structure, and the main chain was linked by a flexible ether bond with a very low $T_{\rm g}$ (182°C). In addition, $T_{\rm g}$ (210°C) of structure III, which was *p*-substituted, was higher than that of structure II because of increased chain rigidity and hindered chain segmentation motion. Similar results have been published by Liaw and Chang [34] regarding different $T_{\rm g}$ values obtained for PI *m*- and *p*-isomers.

With respect to structural isomers IV and V, the chain structure of the m-substituted isomer IV exhibited a lower $T_{\rm g}$ (190°C) than that of isomer V owing to easy segmentation motion. Conversely, the p-substituted isomer V showed a higher $T_{\rm g}$ (225°C) than that of the m-substituted structure IV owing to higher chain rigidity and hindered segmental motion. Overall, structures IV and V exhibited higher $T_{\rm g}$ values than those of structures II and III, respectively, most likely because the bulky SO₂ group inhibits chain segmental motion and increases the thermal energy required

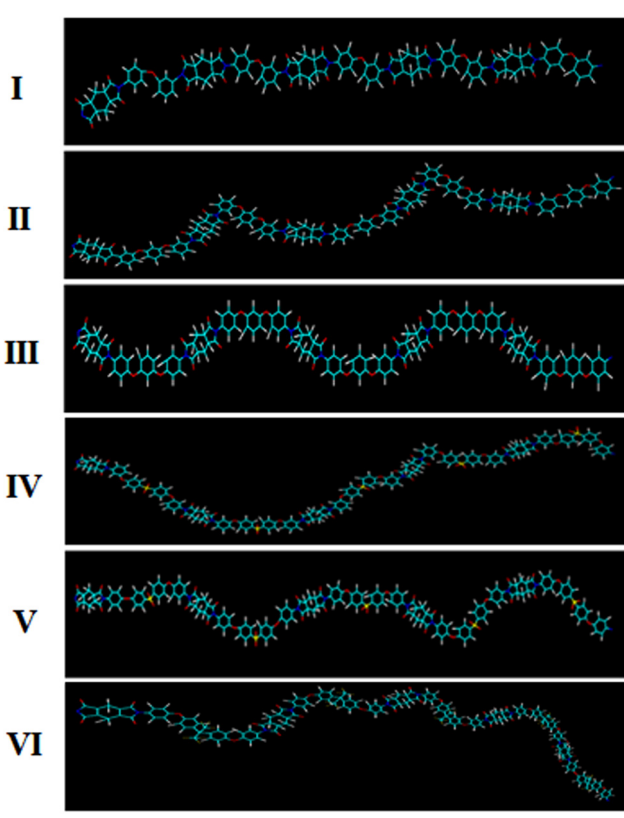


Figure 4: Comparison of the CPI three-dimensional chemical structures with various diamines.

for the chain movement. In the p-substituted structure VI, $T_{\rm g} = 223^{\rm o}$ C was observed as the linear structure of the main chain increased the chain stiffness and because the movement of the entire main chain was hindered by the bulky $-{\rm CF_3}$ substituent. Figure 5 shows the correlation of the DSC thermal curves to the monomer structure leading to various CPI films.

Thermal stability results obtained with TGA are shown in Figure 6, whereas the initial decomposition temperature

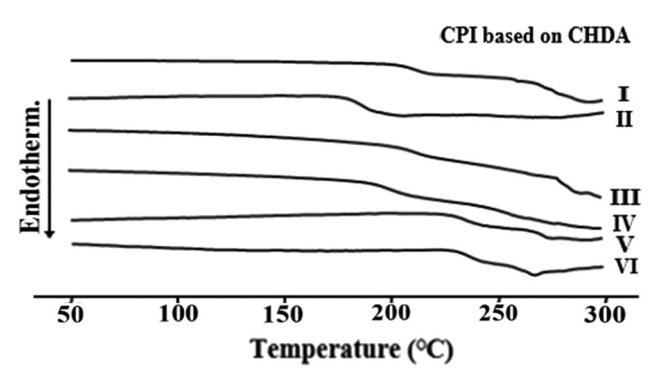


Figure 5: DSC thermograms of the CPI films obtained from the CHDA monomer.

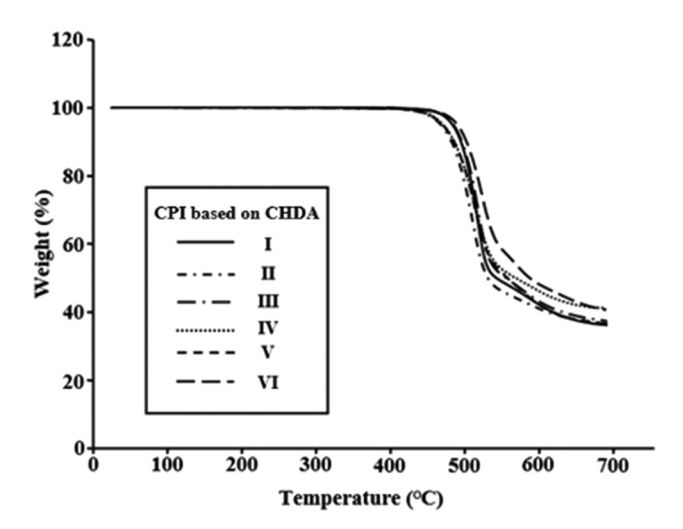


Figure 6: TGA thermograms of the CPI films obtained from the CHDA monomer.

 (T_D^i) and the weight residue at 600°C (wt_R⁶⁰⁰) derived from the thermograms are summarized in Table 2. For each structure, T_D^i was in the range of 449–473°C and wt_R⁶⁰⁰ in the range of 41–48%. The thermal stability was comparable to the previously described $T_{\rm g}$ results. The II, IV, and V structures, in which the main chain was bent in an m-shape or the –SO₂– group was introduced, exhibited relatively low values of T_D^i (449–452°C). In addition, the –SO₂– group can be easily decomposed into radicals due to the steric hindrance and conformational energy caused by high torsion at high temperature [35]. Therefore, the CPI containing the –SO₂– group showed a generally low T_D^i value.

In contrast, linear structure I and p-isomeric structure III exhibited relatively high thermal stability (469°C) because the facilitated chain–molecular–packing allowed the molecular bonding between the main polymer chains (see Figure 4). Despite its curved chain shape, structure VI exhibited the highest T_D^i (473°C) and $\operatorname{wt}_R^{600}$ (48%), owing to the presence of thermally stable –CF₃ substituents (see Table 2).

CTE indicated the linear expansion degree (ppm- $^{\circ}$ C⁻¹) with respect to the temperature change during heating. For all CPI films, CTE was measured in a temperature range below $T_{\rm g}$, namely, from 50 to 150 $^{\circ}$ C. Structure I, the shortest and simplest structure under investigation, exhibited a relatively low value (47.74 ppm- $^{\circ}$ C⁻¹) due to the large number of benzene components, characterized by intrinsic high thermal stability. Structures II and III showed relatively large values (52.61 and 51.41 ppm- $^{\circ}$ C⁻¹, respectively) due to the simple ether bonded structure with relatively low benzene content and low thermal stability. Structures IV and V showed relatively low values

(45.43 and 48.68 ppm·°C⁻¹, respectively) due to the influence of the highly electronegative sulfone group [36,37]. However, as reported in Table 2, CTE values for structures I–V were comparable. Conversely, structure VI showed the largest CTE value (60.37 ppm·°C⁻¹) due to the curved structure caused by the large –CF₃ substituent, which hindered the molecule packing (Figure 4). Figure 7 shows TMA results for CPI films obtained from various monomers.

3.4 Oxygen barrier properties

The polymer–film gas permeability is greatly influenced by several factors, including gas solubility and diffusion, other inherent gas properties, molecular packing, polymer chain interaction, and interaction between polymer chain and gas [38,39]. A crystalline structure characterized by excellent chain packing properties increases the gas barrier properties due to the longer path through which the gas passes compared to an amorphous structure [40,41]. Nevertheless, gas barrier properties were improved for polymer structures interacting with the gas. Table 2 summarizes O₂TR results for CPI films obtained from the monomer structures.

CPI structures I–V showed very low gas permeability $(0.39-2.62 \, \text{cc·m}^{-2} \cdot \text{day}^{-1})$ due to the excellent structure stacking compared to other polymers (see Table 2). In the overall structure, although the main chain contains a meta-structure or SO₂ group, most of the oxygen permeability showed a small value of less than $3.02 \, \text{cc·m}^{-2} \cdot \text{day}^{-1}$ because of the well stacking of molecular chains. However, structure VI, synthesized with 2,2-bis[4-(4-aminophenoxy)

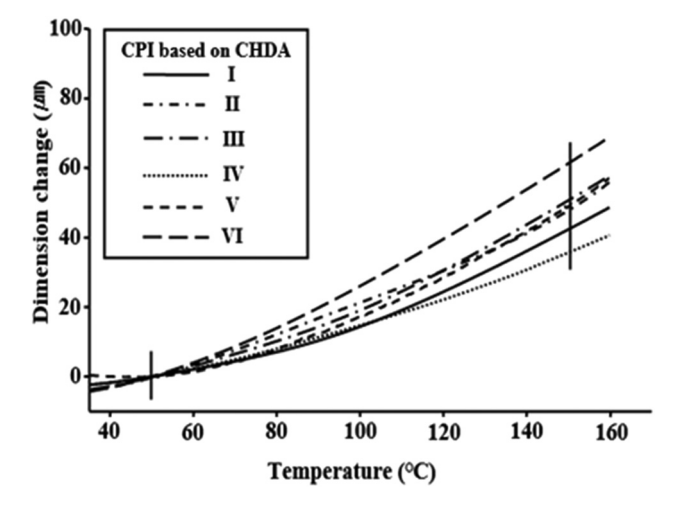


Figure 7: TMA thermograms of the CPI films obtained from the CHDA monomer.

phenyl]hexafluoropropane as the diamine, is totally bent, and the bulky $-CF_3$ substituent interferes with the chain packing, resulting in a high gas permeability $(13.692\,\text{cc}\cdot\text{m}^{-2}\cdot\text{day}^{-1})$. Conclusively, these results are consistent with the CTE outcome.

3.5 Mechanical properties

The ultimate strength, initial modulus, and elongation percent at break (EB) of the CPI I-VI structures were measured using UTM. Results are presented in Table 4. The ultimate strength and initial modulus of structures I-III (88–91 MPa and 3.05–3.14 GPa, respectively), without a substituent in the main chain, showed relatively better mechanical properties compared to structures IV-VI (70–72 MPa and 2.27–2.62 GPa, respectively), bearing $-SO_2$ - and $-CF_3$. Specifically, on average, structures I-III showed better ultimate strength and initial modulus (approximately 27 and 26%, respectively) compared to IV-VI structures. The superior mechanical properties are attributed to the shorter length, more compact molecular packing, and attraction between the CPI structure chains without substituents. For each structure, EB was constant (approximately 3-5%), without a noticeable difference.

3.6 Optical transparency

In this study, UV-Vis. and yellow index (YI) were measured according to the diamine monomer of the prepared CPI film. The UV-Vis. transmittance of the synthesized CPI films is shown in Figure 8, and results are summarized in Table 5. The cutoff wavelength (λ_o) value of all films is less than 310 nm, with the light transmission

Table 4: Mechanical properties of CPI films obtained from the CHDA monomer

СРІ	Ult. Str. (MPa)	Ini. Mod. (GPa)	E.B. ^a (%)
ı	88	3.05	3
II	91	3.14	3
Ш	91	3.13	5
IV	70	2.54	2
V	72	2.62	3
VI	72	2.27	4

^aElongation percent at break.

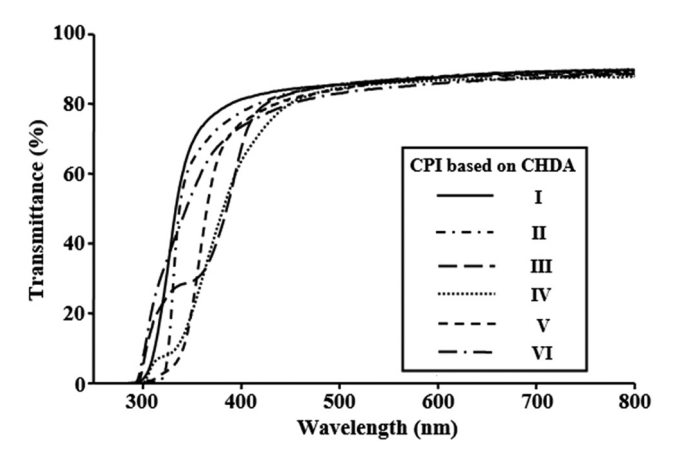


Figure 8: UV-Vis transmittance of various CPI films obtained from the CHDA monomer.

occurring out of the visible region. The transmittance at 550 nm showed excellent optical properties of almost 85–87%, regardless of the monomer structure. Compared to the currently available Kapton® 200KN [42], characterized by a transmittance <60% at 550 nm, our results are particularly good. The measured transmittance is ascribed to the use of a monomer structure interfering with the CTC effect in the main chain.

YI values are listed in Table 5. All CPI structures showed colorless and transparent optical properties, with YI mostly in the range 2.2-4.1 Structures IV and VI showed very low YI values (2.3 and 2.2, respectively) compared to other structures. Furthermore, structure IV showed a lower YI value owing to the hindered effective chain packing due to the overall bent m-structure, compared to other structures. Moreover, structure VI showed a low YI value by reducing the CTC effect because the strong electron-withdrawing groups ($-CF_3$) included in the main chain attracted π electrons and hindered the electron movement [43,44]. Photographs of the prepared CPI films are shown in Figure 9 with the logo image in the background. There was a slight

Table 5: Optical properties of CPI films obtained from the CHDA monomer

СРІ	λ_0^{a}	550 nm ^{trans} (%)	Y.I. ^b	
I	295	86	3.1	
II	310	86	4.0	
III	295	86	4.1	
IV	303	87	2.3	
V	308	86	4.0	
VI	294	85	2.2	

^aYellow index.

^bCut off wave length.

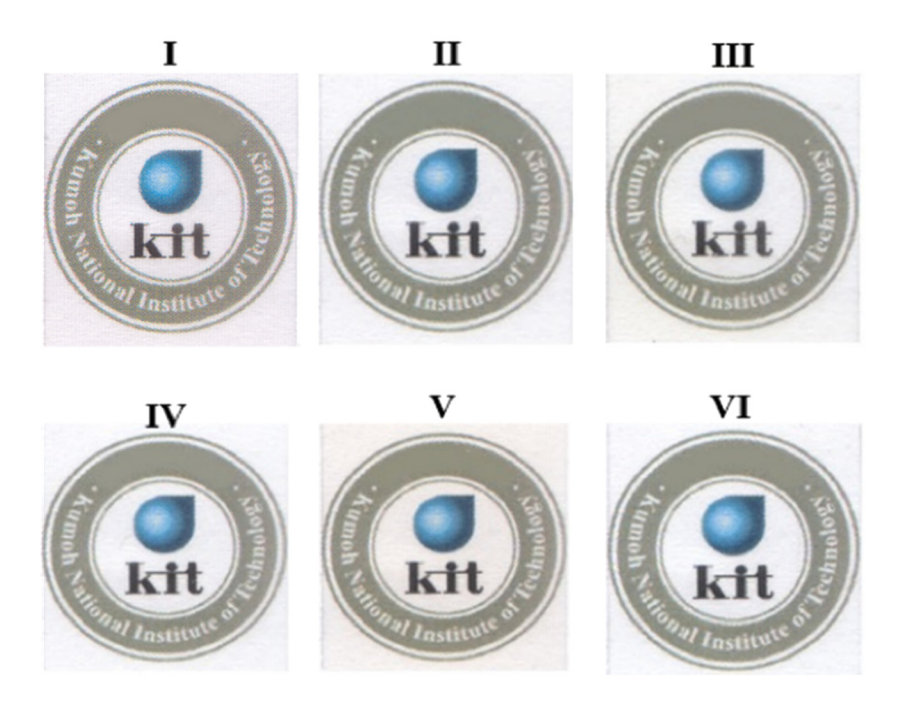


Figure 9: Photographs of the prepared CPI films.

difference in color depending on the type of monomer, whereas the transparency was comparable for all samples.

3.7 Solubility

Typically, CPI materials are special polymers with strong heat and chemical resistance. Particularly, most of their structures are composed of benzene and an alicyclic structure at the end, hampering their melting at high temperatures and chemical dissolution in strong solvents. Therefore, despite the excellent physical properties, the CPI use as an engineering polymer is very limited. The effects of solubility on the film processing ability make the selection of the proper solvent crucial [45,46]. The solubility of CPI films synthesized in this study was measured in various solvents, as shown in Table 6.

All investigated CPI samples did not completely dissolve in general purpose solvents such as acetone, chloroform, methyl alcohol, and toluene. However, the solubility was particularly high in DMAc and DMF and good in dimethyl sulfoxide (DMSO) and N-methyl-2-pyrrolidone (NMP). In addition, weak solubility was observed in methylene chloride and pyridine, whereas some structures were not dissolved at all. Therefore, CPI films were not dissolved in common solvents, while they showed very high solubility in polar solvents.

Specifically, structure I exhibited the lowest solubility, due to the simple and short benzene structure leading to the excellent chain accumulation hindering solvent penetration. Conversely, structure VI showed the best solubility due to the limited chain packing brought about the bulky -CF₃ substituent, causing facile solvent penetration [47,48]. These structural considerations were consistent with the

Table 6: Solvent tests of CPI films obtained from the CHDA monomer

СРІ	Act	CHCl₃	CH ₂ Cl ₂	DMAc	DMF	DMSO	CH₃OH	NMP	Ру	THF	Tol
ı	×	×	×	Δ	Δ	0	×	0	Δ	×	×
II	×	×	Δ	0	0	0	×	0	×	×	×
Ш	×	×	Δ	0	0	0	×	0	×	×	×
IV	×	×	×	0	0	0	×	0	Δ	×	×
V	×	×	Δ	0	0	0	×	0	Δ	×	×
VI	×	×	©	0	0	0	×	0	0	©	×

©: excellent, O: good, Δ: poor, ×: very poor. Act: Acetone, DMAc: N,N-dimethylacetamide, DMF: N,N-dimethylformamide, DMSO: dimethyl sulfoxide, NMP: N-methyl-2-pyrrolidone, Py: pyridine, THF: tetrahydrofuran, Tol: toluene.

measurements of thermomechanical properties and oxygen permeability outcome and coherent with the three-dimensional chain structures as shown in Figure 4.

have read and agreed to the published version of the manuscript.

Conflict of interest: The authors declare no conflict of interest.

4 Conclusions

In this study, CPI films with excellent optical properties were prepared by reacting CHDA dianhydride with six different diamine monomers, including -SO₂- and -CF₃containing structures and *m*- or *p*-isomer structures. The synthesized CPI films were further investigated. Their thermo-mechanical and optical properties were related to the monomer structure, whereas their physical properties were analyzed in view of the diamine monomer structure. Comparing the prepared films shows that the structure including the -CF₃ substituent (structure VI) showed a good thermal stability, excellent optical transparency, and easy solubility. Conversely, it showed the poor results in CTE, gas barrier properties, and mechanical properties due to the poor chain packing. However, all of the produced films exhibited excellent optical transparency, with $YI \leq 4.1$.

The newly synthesized CPI films in this study can be inexpensively mass-produced and used in flexible display films, solar panel substrates, or rollable and wearable devices that require excellent thermo-mechanical properties and colorless and transparent optical properties. CPI is a promising polymeric material that can replace glass in several material science fields.

Acknowledgment: This research was supported by the Basic Science Research Program through the National Research Foundation of Korea (NRF) funded by the Ministry of Education (2016R1A6A1A03012069). This work also was supported by the National Research Foundation of Korea (NRF) grant funded the Korea government (MSIT) (2022R1A2C1009863).

Funding information: This research was supported by the Basic Science Research Program through the National Research Foundation of Korea (NRF) funded by the Ministry of Education (2016R1A6A1A03012069). This work also was supported by the NRF of Korea grant funded the Korea government (MSIT) (2022R1A2C1009863).

Author Contributions: J.-H. Chang designed the project and wrote the manuscript. L.K. Kwac and H.G. Kim reviewed and data analyzed. H. Jeon prepared the samples and participated in the data analysis. All authors

References

- Cheng, S. H., S. H. Hsiao, T. H. Su, and G. S. Liou. Novel aromatic poly(amine-imide)s bearing a pendent triphenylamine group: synthesis, thermal, photophysical, electrochemical, and electrochromic characteristics. Macromolecules, Vol. 38, 2005, pp. 307-316.
- Liou, G. S. and S. H. Hsiao. Synthesis and properties of new organosoluble and alternating aromatic poly(ester-amideimide)s with pendant phosphorus groups. Journal of Polymer Science Part A Polymer Chemistry, Vol. 39, 2001, pp. 1786-1799.
- Liaw, D.-J., K.-L. Wang, Y.-C. Huang, K.-R. Lee, J.-Y. Lai, and C.-S. Ha. Advanced polyimide materials: Syntheses, physical properties and applications. Progress in Polymer Science, Vol. 37, 2012, pp. 907-974.
- Shinji, A., M. Tohru, and S. Shigekuni. Coloration of aromatic polyimides and electronic properties of their source materials. Polymer Journal, Vol. 29, 1997, pp. 69-76.
- Guo, Y., H. Qiu, K. Ruan, Y. Zhang, and J. Gu. Hierarchically multifunctional polyimide composite films with strongly enhanced thermal conductivity. Nano-Micro Letters, Vol. 14, No. 26, 2022, pp. 1-13.
- Ruan, K., Y. Guo, and J. Gu. Liquid crystalline polyimide films with high intrinsic thermal conductivities and robust toughness. Macromolecules, Vol. 54, 2021, pp. 4934-4944.
- Chen, C.-J., H.-J. Yen, Y.-C. Hu, and G.-S. Liou. Novel programmable functional polyimides: Preparation, mechanism of CT induced memory, and ambipolar electrochromic behavior. Journal of Materials Chemistry C: Materials for Optical and Electronic Devices, Vol. 1, 2013, pp. 7623-7634.
- Nishihara, M., L. Christiani, A. Staykov, and K. Sasaki. Experimental and theoretical study of charge-transfer complex hybrid polyimide membranes. Journal of Polymer Science Part B Polymer Physics, Vol. 52, 2014, pp. 293-298.
- Chang, J.-H. Equibiaxially stretchable colorless and transparent polyimides for flexible display substrates. Reviews on Advanced Materials Science, Vol. 59, 2020, pp. 1-9.
- [10] Shin, H. I., Y.-J. Kwark, and J.-H. Chang. Colorless and transparent copolyimides and their nanocomposites: Thermooptical properties, morphologies, and gas permeabilities. Polymers, Vol. 11, 2019, pp. 1-17.
- [11] Shahram, M. A. and H. Mehdi. Synthesis and characterization of novel heat resistant poly(amide imide)s. European Polymer Journal, Vol. 41, 2005, pp. 2010-2015.
- [12] Yang, C. Y., S. L. C. Hsu, and J. S. Chen. Synthesis and properties of 6FDA-BisAAF-PPD copolyimides for microelectronic applications. Journal of Applied Polymer Science, Vol. 98, 2005, pp. 2064-2069.

- [13] Kim, J.-C. and J.-H. Chang. Quaternary copolyimides with various monomer contents: Thermal property and optical transparency. *Macromolecular Research*, Vol. 22, 2014, pp. 1178–1182.
- [14] Choi, I. H. and J.-H. Chang. Characterization of colorless and transparent polyimide films synthesized with various amine monomers. *Polymer(Korea)*, Vol. 34, 2010, pp. 480–484.
- [15] Kim, Y. and J.-H. Chang. Colorless and transparent polyimide nanocomposites: Thermo-optical properties, morphology, and gas permeation. *Macromolecular Research*, Vol. 21, 2013, pp. 228–233.
- [16] Choi, I. H. and J.-H. Chang. Fabrications and properties of colorless polyimide films depend on various heat treatment conditions via crosslinkable monomer. *Polymer(Korea)*, Vol. 34, 2010, pp. 391–397.
- [17] Hasegawa, M., K. Ichikawa, S. Takahashi, and J. Ishii. Solution-processable colorless polyimides derived from hydrogenated pyromellitic dianhydride: Strategies to reduce the coefficients of thermal expansion by maximizing the spontaneous chain orientation behavior during solution casting. *Polymers*, Vol. 14, No. 1131, 2022, pp. 1–30.
- [18] Choi, M.-C., Y. Kim, and C.-S. Ha. Polymers for flexible displays: From material selection to device applications. *Progress in Polymer Science*, Vol. 33, 2008, pp. 581–630.
- [19] Burrows, P. E., G. L. Graft, M. E. Gross, P. M. Martin, M. K. Shi, M. Hall, et al. Ultra barrier flexible substrates for flat panel displays. *Displays*, Vol. 22, 2001, pp. 65–69.
- [20] Chiang, C.-J., C. Winscom, S. Bull, and A. Monkman. Mechanical modeling of flexible OLED devices. *Organic Electronics*, Vol. 10, 2009, pp. 1268–1274.
- [21] Shen, Y., Z. Feng, and H. Zhang. Study of indium tin oxide films deposited on colorless polyimide film by magnetron sputtering. *Materials and Design*, Vol. 193, 2020, id. 108809.
- [22] Lozano, A. E., J. D. Abajo, J. G. de la Campa, C. Guillén, J. Herrero, and M. T. Gutiérrez. Thin-film polyimide/indium tin oxide composites for photovoltaic applications. *Journal of Applied Polymer Science*, Vol. 103, 2007, pp. 3491–3497.
- [23] Morikawa, H. and M. Fujita. Crystallization and electrical property change on the annealing of amorphous indium-oxide and indium-tin-oxide thin films. *Thin Solid Films*, Vol. 359, 2000, pp. 61–67.
- [24] Choi, S.-J., S.-J. Kim, and I.-D. Kim. Ultrafast optical reduction of graphene oxide sheets on colorless polyimide film for wearable chemical sensors. NPG Asia Materials, Vol. 8, 2016, id. e315.
- [25] Xu, T., D. Kong, H. Tang, X. Qin, X. Li, A. Gurung, et al. Transparent MoS2/PEDOT composite counter electrodes for bifacial dye-sensitized solar cells. ACS Omega, Vol. 5, 2020, pp. 8687–8696.
- [26] Jitsuo, O., H. Sotaro, and K. Shuta. Process and apparatus for production of colorless transparent resin film. *U.S. Patent* 8,357,322, 2013.
- [27] Jitsuo., O., M. Takashi, K. Ko, and K. Shuta. Process for producing polyimide film. *U.S. Patent* 7,871,554, 2011.
- [28] Pavia, D. L., G. M. Lampman, G. S. Kriz, and J. A. Vyvyan. Introduction to spectroscopy, Chap. 2, Cengage Learning: Boston, Massachusetts, USA, 2008, pp. 14–95.
- [29] Pavia, D. L., G. M. Lampman, G. S. Kriz, and J. A. Vyvyan. Introduction to Spectroscopy, Chap. 4, Cengage Learning:, Boston, Massachusetts, USA, 2008, pp. 146–183.

- [30] Agag, T. and T. Takeichi. Polybenzoxazine-montmorillonite hybrid nanocomposites: Synthesis and characterization. *Polymer*, Vol. 41, 2000, pp. 7083-7090.
- [31] Fornes, T. D., P. J. Yoon, D. L. Hunter, H. Keskkula, and D. R. Paul. Effect of organoclay structure on nylon 6 nanocomposite morphology and properties. *Polymer*, Vol. 43, 2002, pp. 5915–5933.
- [32] Chang, J.-H., B.-S. Seo, and D.-H. Hwang. An exfoliation of organoclay in thermotropic liquid crystalline polyester nanocomposites. *Polymer*, Vol. 43, 2002, pp. 2969–2974.
- [33] Ju, J. and J.-H. Chang. Characterizations of poly(ester imide) nanocomposites containing organically modified hectorite. *Macromolecular Research*, Vol. 22, 2014, pp. 549–556.
- [34] Liaw, D.-J. and F.-C. Chang. Highly organosoluble and flexible polyimides with color lightness and transparency based on 2,2-bis[4-(2-trifluoromethyl-4-aminophenoxy)-3,5-dimethyl-phenyl] propane. *Journal of Polymer Science Part A Polymer Chemistry*, Vol. 42, 2004, pp. 5766–5774.
- [35] Butt, M. S., X. Akhtar, M. Z. Zaman, and A. Munir. Synthesis and characterization of some novel aromatic polyimides. *European Polymer Journal*, Vol. 41, 2005, pp. 1638–1646.
- [36] Numata, S., S. Oohara, K. Fujisaki, J. Imaizumi, and N. Kinjo. Thermal expansion behavior of various aromatic polyimides. *Journal of Applied Polymer Science*, Vol. 31, 1986, pp. 101–110.
- [37] Liou, H.-C., P. S. Ho, and R. Stierman. Thickness dependence of the anisotropy in thermal expansion of PMDA-ODA and BPDA-PDA thin films. *Thin Solid Films*, Vol. 339, 1999, pp. 68-73.
- [38] Jarus, D., A. Hiltner, and E. Baer. Barrier properties of polypropylene/polyamide blends produced by microlayer coextrusion. *Polymer*, Vol. 43, 2002, pp. 2401–2408.
- [39] LeBaron, P. C., Z. W. Wang, and T. J. Pinnavaia. Polymer-layered silicate nanocomposites: An overview. *Applied Clay Science*, Vol. 15, 1999, pp. 11–29.
- [40] Kim, J. H., W. J. Koros, and D. R. Paul. Physical aging of thin 6FDA-based polyimide membranes containing carboxyl acid groups. Part I. Transport properties. *Polymer*, Vol. 47, 2006, pp. 3094–3103.
- [41] Min, U. and J.-H. Chang. *Thick films: Properties, technology and applications*, Chapter 5, I. P. Panzini, ed, Nova Sci. Publisher Inc, New York, 2012, pp. 261–282.
- [42] Hasegawa, M. and K. Horie. Photophysics, photochemistry, and optical properties of polyimides. *Progress in Polymer Science*, Vol. 26, 2001, pp. 259–335.
- [43] Ma, S. L., Y. S. Kim, J. H. Lee, J. S. Kim, I. Kim, and J. C. Won. Synthesis and properties of colorless polyimide and its nanocomposite for plastic display substrate. *Polymer(Korea)*, Vol. 29, 2005, pp. 204–210.
- [44] Yang, C.-Y., S. L.-C. Hsu, and J. S. Chen. Synthesis and properties of 6FDA-BisAAF-PPD copolyimides for microelectronic applications. *Journal of Applied Polymer Science*, Vol. 98, 2005, pp. 2064–2069.
- [45] Ghaemy, M., R. Porazizollahy, and M. Bazzar. Novel thermal stable organosoluble polyamides and polyimides based on quinoxalin bulky pendent group. *Macromolecular Research*, Vol. 19, 2011, pp. 528–536.
- [46] Kim, M. H., M. H. Hoang, D. H. Choi, M. J. Cho, H. K. Ju, D. W. Kim, et al. Electro-optic effect of a soluble nonlinear optical polyimide containing two different chromophores with different sizes in the side chain. *Macromolecular Research*, Vol. 19, 2011, pp. 403–407.

- [47] Yang, C.-P., R.-S. Chen, and K.-H. Chen. Organosoluble and light-colored fluorinated polyimides based on 2,2-bis[4-(4-amino-2-trifluoromethylphenoxy)phenyl]propane and aromatic dianhydrides. *Journal of Applied Polymer Science*, Vol. 95, 2005, pp. 922–935.
- [48] Maya, E. M., A. E. Lozano, J. Abajo, and J. G. Campa. Chemical modification of copolyimides with bulky pendent groups: Effect of modification on solubility and thermal stability. *Polymer Degradation and Stability*, Vol. 92, 2007, pp. 2294–2299.